DEEP LEARNING SURROGATE MODEL FOR ROTORCRAFT AEROACOUSTIC SIMULATIONS USING A GEODESIC CONVOLUTIONAL NETWORK

Bianca Erwee, Leonardo Helicopters, Bristol, UK
Alessandro Scandroglio, Leonardo Helicopters, Milan, Italy
Nicoletta Sanguini, Leonardo Helicopters, Milan, Italy
Tommaso Benacchio, Leonardo Helicopters, Milan, Italy
Francesco di Cintio, Leonardo Helicopters, Milan, Italy

Abstract

This paper presents a new state of the art surrogate assisted aeroacoustics toolchain, with a deep learning surrogate model able to accurately predict blade pressure distributions for helicopter main rotors in various flight conditions. By training a state of the art geodesic convolutional neural network, the surrogate model is able to accurately predict new cases in 0.1s with an R^2 of 99% - 10,000 faster than the existing tool. Surrogate models have been built for four LH platforms, and a multi-blade model developed which showed very promising rotor performance predictions for an unseen blade design. The helicopter aeroacoustic tool chain can now run in just 8 minutes, down from 8 hours. In future work, the training of the surrogate models will be extended, to consider a wider flight envelope of flight conditions, and grow its ability to predict unseen rotor blade performance.

1 NOTATION

Acronyms:

ERF	European Rotorcraft Forum
ACARE	Advisory Council for Aviation Research
CNN	Convolutional Neural Networks
GCNN	Geodesic Convolutional Neural Network
NN	Neural Network
TPP	Tip Path Plane
FWH	Ffowcs Williams Hawkings
CVC	Constant Vorticity Contour
BVI	Blade Vortex Interaction
LH	Leonardo Helicopters
OASPL	Overall Sound Pressure Level

2 INTRODUCTION

The conventional helicopter configuration (or ‘Penny Farthing’ design) is known for its highly characteristic noise signature, often associated with noise pollution and annoyance among the general public [1]. This brings a challenge to the rotorcraft design community, as in tandem, public expectation of reduced environmental impact on community noise around airports increases [2]. This is compounded by governmental initiatives, such as the European Union Vision for 2025, and the Advisory Council for Aviation Research (ACARE) which have both set goals for progress in the reduction of perceived aircraft noise emissions [2]. The ACARE goal for rotorcraft external noise reduction has been set at 50%.

The importance of reducing external helicopter noise is therefore widely undisputed [3], and perhaps as a result there are now numerous research initiatives aiming to reduce rotorcraft noise, both by actively changing helicopter design and by optimising the operational use of rotorcraft to reduce on ground noise footprints [1] [4]. In order to predict and optimise on-ground helicopter noise LH currently uses an aeroacoustic toolchain, using our mid fidelity aerodynamics solver EMAA. An accurate model of helicopter rotor noise is dependent on an aerodynamic solver – such as EMAA – which is capable of accurately predicting the wake structure of the rotor, and the resulting pressure fluctuations over the blades caused by vortices interacting with the rotor blades.

However, running the aerodynamic simulation for a single flight condition can take up to 8 hours to run. The capabilities of optimisation loops for rotor aeroacoustic & aerodynamic performance are therefore stunted by the computational time required to run them [5]. The same challenge is met performing acoustic trajectory optimisations, designed to optimise helicopter flight trajectories to lower on ground noise [1]. These tools require large acoustic hemisphere databases, owing to the inherent non-linearity of helicopter acoustic behaviour with changes in flight condition. For velocity and flight path angle, for example, databases typically need to be generated in 10kt and 1º steps respectively, as a minimum. As a result databases of at least 60 different flight trajectories are needed. These take a large amount of time and resources to generate, owing predominantly to the computational cost of the aerodynamic solver within the aeroacoustic toolchain.

The challenge, then, is to consider how the issue of computational time in this aeroacoustic toolchain might be overcome. In recent years, the exponential build in computational power and surrogate modelling techniques has resulted in a boom of innovation, as the application of surrogate modelling techniques to engineering design opens up a host of new possibilities, particularly with regard to optimisation & multidisciplinary applications [2] [6]. The application of deep learning to engineering design is a game changer for the industry – allowing the rapid acceleration of design processes reliant on computationally expensive simulations, without the previously necessary reduction in simulation fidelity, or availability of massive computational power [7].

The emergence of Convolutional Neural Networks (CNN), which allows the learning of task specific features from examples have, in particular, sparked the beginning of a revolution in engineering design. In 2015, Masci et al proposed Geodesic Convolutional Neural Networks (GCNNs): an extension of the CNN paradigm to non-Euclidean manifolds based on local geodesic coordinates that are analogous to 'patches' in images. GCNNs are capable of dealing with 3D shape analysis, and more importantly are generalizable (can be trained on one set of shapes, and applied to another) [8]. Utilising shape optimisation in the application of such a model to helicopter rotor blades could have powerful capabilities, not just in terms of aerodynamics, but potentially also in opening the door to multidisciplinary analysis, considering vibration, aero elasticity & composite structural blade design [6] [9].

This paper therefore presents a newly developed, state of the art GCNN deep learning surrogate model, able to accurately predict the blade pressure distribution previously calculated by the aerodynamic solver. This pressure distribution is used to calculate the rotor loading over the rotor Tip Path Plane (TPP), which our Ffowcs Williams Hawkings (FWH) tool requires to propagate the near field noise sources to a hemisphere of microphones. The surrogate tool is designed to output the data in a format directly readable by our in-house FWH tool, allowing seamless integration within our existing aeroacoustics toolchain.

3 AEROACOUSTIC TOOLCHAIN

3.1 Current Toolchain

Leonardo currently uses an aeroacoustic toolchain, as shown graphically below in Figure 1. The key solvers include a flight mechanics solver, an aerodynamics solver, a far field acoustics solver able to calculate the rotor noise sources and propagate the noise to a hemisphere surrounding the aircraft, and a far field noise propagation tool which predicts the on-ground noise of the helicopter.

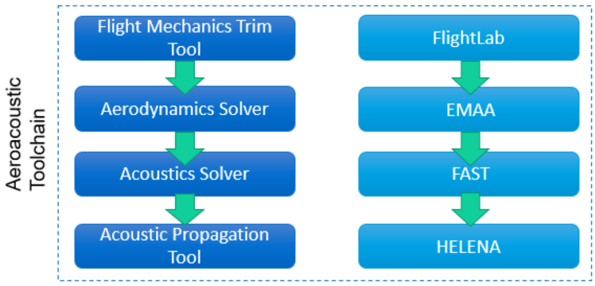

Figure 1: Aeroacoustic toolchain

The flight mechanics tool, FlightLab, is used to predict the steady state trim condition of the rotor for a given flight condition – the resulting pitching and flapping angles of the rotor, in conjunction with the overall attitude of the aircraft, are then passed to the aerodynamics tool.

Using these inputs, the aerodynamics solver is able to reconstruct the steady-state motion of the blade, and predict the aerodynamic performance of the rotor. The toolchain uses a state of the art mid-fidelity aerodynamics solver called EMAA, an unsteady free wake panel method, which uses a Constant Vorticity Contour (CVC) wake implementation. An example of the graphical output from this physics based tool can be seen below in Figure 2. The tool is able to simulate the flow conditions necessary to predict thickness, loading and importantly also Blade Vortex Interaction (BVI) noise, using the FWH acoustics solver FAST.

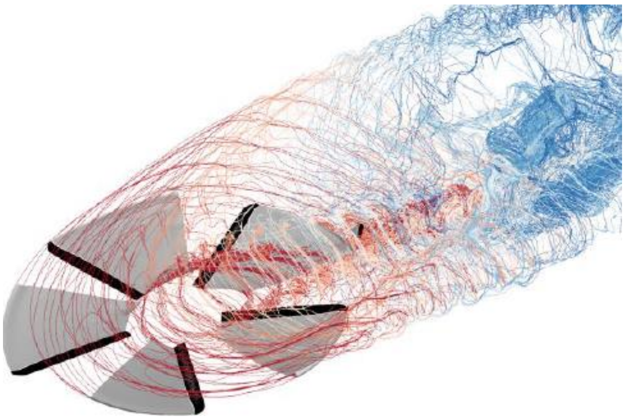

Figure 2: Aerodynamic Solver EMAA Graphical Output

The FWH tool is configured to run using either the compact or non-compact versions of the Farassat 1A formulation, and as such by default the coupled aerodynamics solver, EMAA, will output both formats required by the tool. This can either be:

1. Forces spanwise along the blade, calculated by integrating panel forces in the chord-wise direction. The result is a rotor loading contour plot.
2. Full blade pressure distributions for each 2 degree azimuthal step.

The graphical representations of these inputs are shown below in Figure 3.

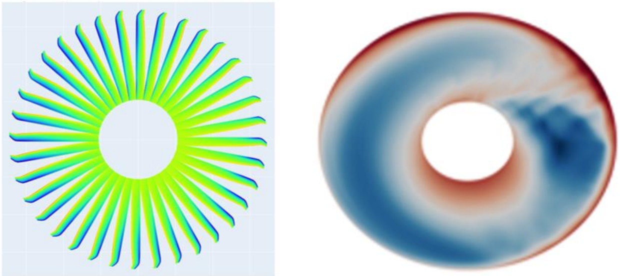

(a) (b)

Figure 3: Graphical representations of the force/pressure inputs required by the FWH acoustics tool for (a) non-compact and (b) compact solutions

The FWH tool is then used to calculate the blade noise sources and propagate the sound to a hemisphere of microphones, as shown graphically below in Figure 4.

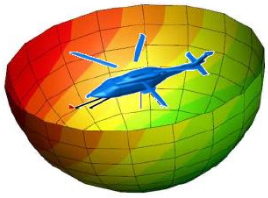

Figure 4: Acoustic Hemisphere output from FWH solver

This hemisphere, calculated for each 1/3 octave band, is then input into our onground propagation solver, HELENA, which propagates the noise to the ground using a simple spherical spreading methodology and calculates the on-ground noise footprint for the aircraft in a given flight trajectory. An example of the calculated footprint is shown below in Figure 5.

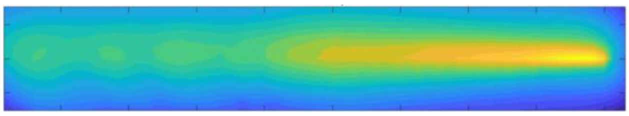

Figure 5: SEL On-Ground Noise Footprint

3.2 Potential of Surrogate Assisted Methodology

In this project, the potential of using surrogate methods to directly predict the acoustic hemispheres and aerodynamic pressures / rotor loads needed by acoustic tool, FAST were investigated. Figure 6 shows graphically the potential changes to the toolchain which were considered.

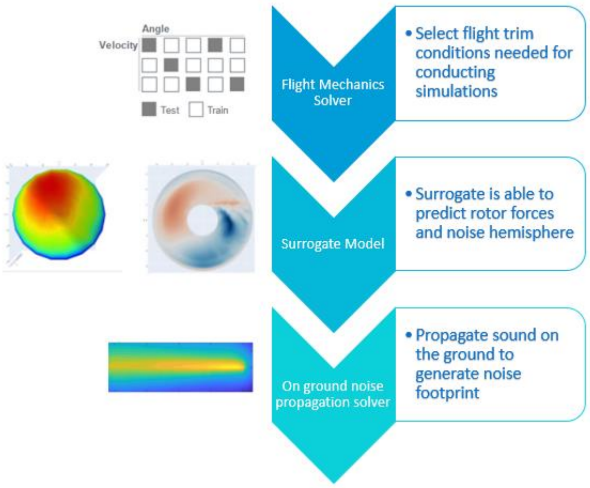

Figure 6: Surrogate Assisted Approach – potential for improvement

However, initial investigations showed that using the state of the art GCNN, which is geared towards the understanding of nodal / edgewise attributes on complex 3D meshes, the surrogate modelling of the aerodynamics outputs showed the greatest potential. Computationally, the aerodynamics solver is by far the most expensive – to run each case, with a minimum level of required computational accuracy, on an HPC takes approximately 8 hours. Comparatively, the flight mechanics tool takes 5 minutes per case, the FWH tool 5 minutes, and HELENA 5 minutes or less, depending on the resolution of on ground microphones required. As such, the mid-fidelity aerodynamics tool is in this case the most critical component of the toolchain. The potential time advantage gained by using a surrogate assisted approach to predict the aerodynamic rotor loads/pressures for the acoustic solver (FAST) is game changing – and would be the key to enabling the optimisation of rotor designs in rapid time scales.

As such, the decision was made to focus on the surrogate modelling of the aerodynamic tool for the aeroacoustic toolchain. To train the aerodynamic surrogate model for the aeroacoustic toolchain, high quality accurate data was needed, covering the flight conditions which the surrogate model would need to handle. In rotorcraft aeroacoustics, large databases of noise hemispheres are generated for noise trajectory optimisations and validation activities. Since the approach condition is the most noise critical condition, where BVI is expected to occur, these databases are usually created for varying descent angles and speeds.

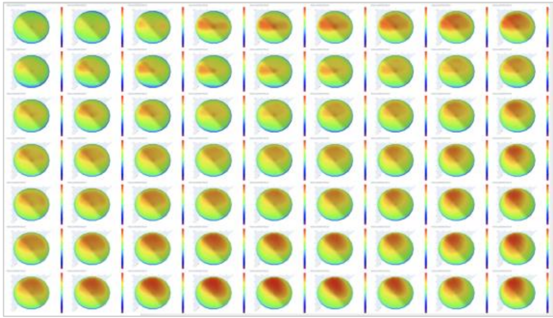

Figure 7: LH Platform 1 Acoustic Hemisphere Database

The presence of BVI related noise within these databases is an additional challenge for the surrogate modelling tool, as the presence of this type of noise source results in a particularly non-linear acoustic database. In the following project, 4 acoustic databases are considered. Two vary with both flight speed and angle of descent in steps of 10kts and 1º respectively, and were the main focus of development in the project. These databases are described as follows:

- Platform 1: 40-100kts, 0-15º, 112 cases
- Platform 2: 50-100kts, 0-15º, 96 cases

In addition, in a multi-blade geometry investigation done at the end of the study, two additional smaller databases were also considered. These vary with both flight speed and angle of descent in steps of 10kts and 4º respectively, as follows:

- Platform 3: 40-100kts, 0-12º, 28 cases
- Platform 4: 40-100kts, 0-12º, 28 cases

4 NEURAL NETWORK & MODELLING ENVIRONMENT

The model developed in this project utilizes a state of the art Geodesic Convolutional Neural Network (GCNN) for 3D deep learning applications.

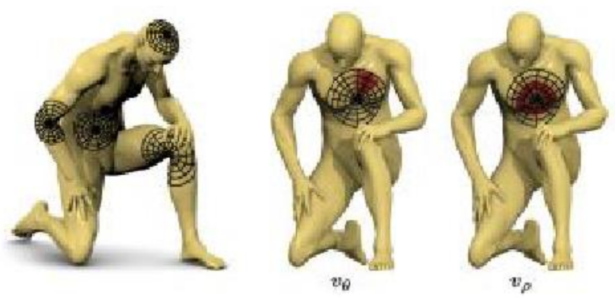

Figure 8: GCNN Polar local geodesic coordinates [10]

GCNNs were first proposed in 2015, by Masci et al [8]; they are an extension of the CNN paradigm to non-Euclidean manifolds based on local geodesic coordinates that are analogous to 'patches' in images (see Figure 8). This model uses local filters, applied to geodesic radial patches as shown below in Figure 9. Within the learning phase of the surrogate model, a gradient descent based optimisation of the convolutional filter is applied, as is standard for CNNs. In addition, predefined Gaussian parameters are learnt, as described by Monti et al [10].

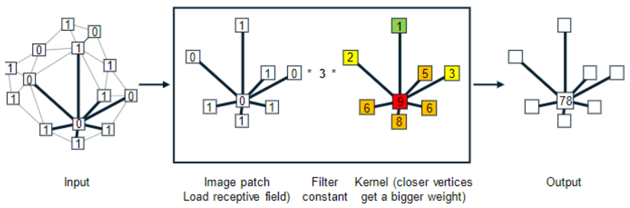

Figure 9: Adaptation of convolutions to take into account the distance between vertices

GCNNs are capable of dealing with 3D shape analysis, and more importantly are generalizable (can be trained on one set of shapes, and applied to another) [8].

The training pipeline is written in python, and fully deployed on Davinci-1, Leonardo's state of the art HPC.

5 INVESTIGATION

The following section details the development stages of the aeroacoustic surrogate assisted toolchain. The first step was to create a working pipeline, and generate initial predictions. From there, the predictions could be assessed and issues / errors in the performance of the surrogate could be addressed. In this initial analysis the Platform 1 dataset was used, an array of 112 cases varying in velocity and descent angle of approach.

The first pipeline was built to directly predict the compact input file required by FAST (as shown graphically in Figure 3b). This allowed the key evaluation of model results, using r2 and L1 error metrics to determine the performance of the model with respect to the physics based model predictions. The input information given to the deep learning surrogate, in addition to the rotor thrust contours (located on the Tip Path Plane (TPP) of the rotor), consisted simply of the flight speed (in kts) and the angle of descent of the helicopter (º). However, given the highly non-linear behaviour of the aeroacoustic database (exacerbated by the BVI noise present in some cases), this initial approach struggled to predict the full database accurately.

It was clear from this initial approach that the surrogate required a more detailed understanding of the motion of the rotor, thus allowing it to identify the relation between the changing steady state motion of the blade, and the resulting pressure distributions of the rotor. To do this, the inputs to the model were increased to include all of the flapping and pitching fourier coefficients, allowing the reconstruction of the blades harmonic motion in 3D space. This adaptation of the model improved its ability to capture the non-linear behaviour of the rotor thrust over the rotor disc.

However, even with the errors minimised (with an r2 of 98%), the results showed that when run through FAST, the directionality of the noise calculated by the physics based model and surrogate based approaches were still showing differences – particularly for certain cases. Further investigation showed that these discrepancies could be correlated with the difference in force gradients predicted by the physics based and surrogate approaches (an example plot can be seen below in Figure 10).

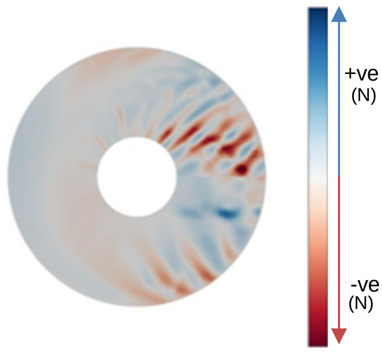

Figure 10: Physics based predictions for Fz Rotor Gradients (Derivative of the Fz with respect to Azimuth Angle), Platform 1

Directly predicting the integrated spanwise forces on the rotor disc, the pressure gradients were being smoothed out by the surrogate model (see Figure 11) , and as a result the acoustic behaviour of the rotor was still different using the surrogate approach. As a result, a second pipeline was developed, to investigate whether directly predicting the pressures on each blade could reduce the error in the gradient predictions.

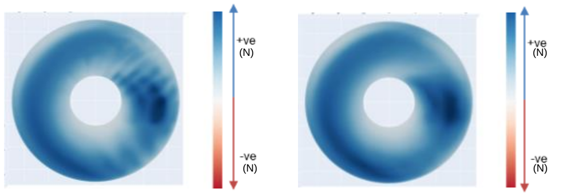

(a) (b)

Figure 11: Pipeline 1 Fz rotor disc contour predictions for (a) physics based solver and (b) surrogate model for 90kts, 9º descent angle. Helicopter nose is pointing left and rotor spinning anticlockwise.

The second pipeline involved training the Neural Network (NN) directly on the non-compact blade pressure distributions (see Figure 3a), and then converting the pressures to forces and integrating chord-wise within the pipeline to output the compact FWH input file. This is advantageous, as the compact formulation of Farassat 1a is computationally considerably faster without any noticeable reduction in performance or accuracy.

The training of the GCNN using complex 3D geometries and pressure distributions made a significant difference to the performance of the surrogate model. It should also be noted that the 112 cases making up the Platform 1 database is a relatively small dataset. Using this second pipeline, it became possible to artificially increase the size of the dataset by a factor of 180, by considering each separate blade pressure distribution, at each azimuthal step, as a separate case.

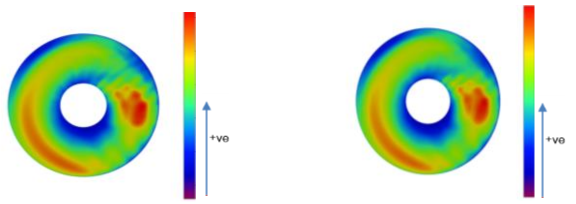

(a) (b)

Figure 12: Pipeline 2 Fz rotor disc contour predictions for (a) physics based solver and (b) surrogate model for 90kts, 9º descent angle

While this data treatment was slightly limited from a test/train perspective (all blades taken from a single flight condition needed to be kept together, in either the test or train sets), the treatment had a huge impact. In this way, it was possible to create an 'artificial' database of 20,160 cases with a test train split of 10:90.

The results from this alternative approach immediately showed an improvement on the previous approach, and the gradients were no longer smoothed out – this is shown in Figure 12.

However, this still left the challenge of accurately predicting the blade pressures. To achieve the highest level of accuracy, an error correlation was calculated by averaging the tests errors across each angle to determine if certain areas were more difficult to predict – this is shown below in Figure 13.

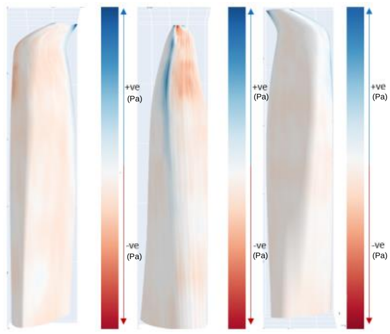

Figure 13: Blade pressure prediction error correlation for the upper surface (left), leading edge (middle) and lower surface (right)

Correlation at the leading edge of the blade indicated the need to target this area to reduce the errors. To do this, a leading edge refinement was applied to the blade. This was done as shown below in Figure 14, using a simple linear interpolation algorithm to generate training data at these 'artificially' created data points.

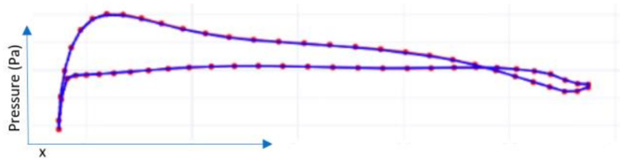

Figure 14: Refined Leading Edge Pressure vs Chord-wise position (x) from the leading edge.

The leading edge refinement significantly reduced the remaining errors in the blade predictions. The final blade predictions, were as shown below for an example case in Figure 15.

In the final step of this initial investigation, the model was retrained and hyper-parameter tuned to achieve a high granularity in the prediction of the forces.

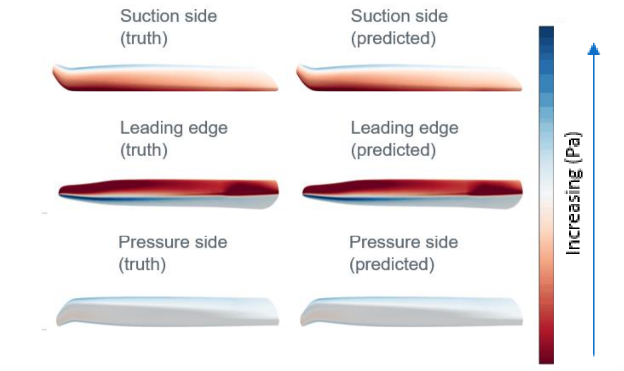

Figure 15: Blade pressure ground truth vs prediction

6 SURROGATE ASSISTED TOOLCHAIN

The final toolchain and pipeline are described in this section.

6.1 Toolchain

With the addition of the surrogate model, the aeroacoustics toolchain now has an updated, surrogate assisted workflow as shown below in Figure 16.

The surrogate tool is designed to output the data in a format directly readable by our in-house FWH tool, allowing seamless integration within our existing aeroacoustics toolchain (See Figure 16). It has also been fully deployed on the Davinci1 high performance cluster.

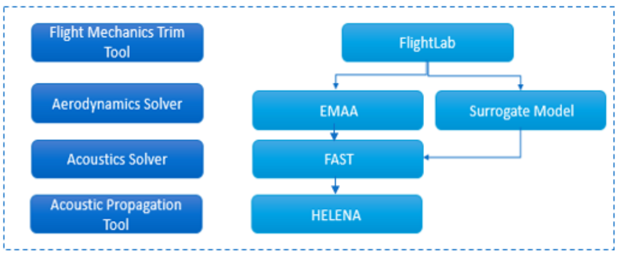

Figure 16: Surrogate Assisted Aeroacoustic Toolchain

The surrogate model uses a GCNN, which is trained using pressure data, mapped to a given blade mesh. A number of scalar parameters are taken from the aerodynamic solver input files for each case, and used to give the surrogate model additional context for its predictions. As such, the inputs used to train the model can be listed as follows:

Scalars: Velocity and angle of descent, flapping and pitching fourier coefficients

Mesh: Blade mesh

Mesh Quantities: Pressure distribution for rotor blade at 2 degree azimuth steps.

6.2 Pipeline Definition

The final pipeline for the surrogate model is as shown below in Figure 17. The pipeline consists of 6 core steps. In the first, the required input parameters needed to train the surrogate are obtained, reading in the rotor trim parameters, speed, angle of descent, the blade mesh file, and associated pressure distribution of the blade in 2 deg azimuth steps.

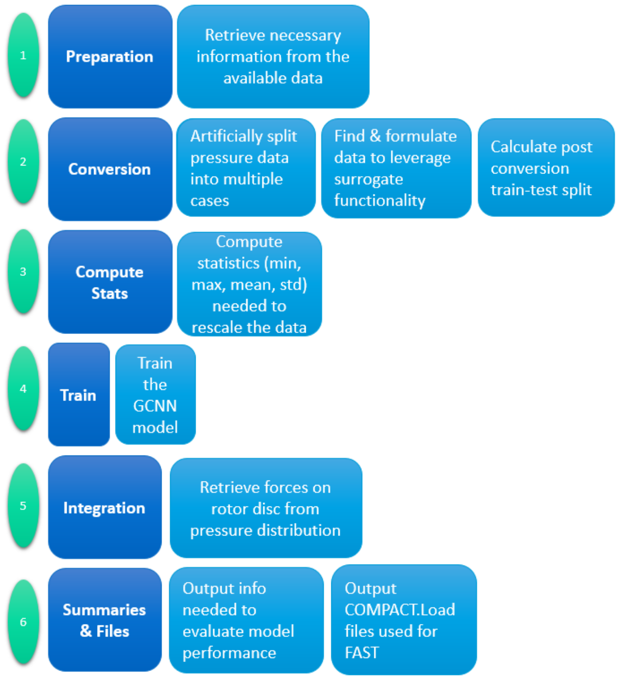

Figure 17: Training Surrogate Methodology

In the conversion step, the inputs required by the NN are reconfigured to data types used by the network – in this case the pressure field and flight condition scalar parameters.

Once converted, the datasets are split between testing and training, and the statistics needed to rescale the data are computed. The GCNN model is then trained on the selected training data (step 4) and the data converted to the format required by FAST (steps 5 &6). A number of summary files are generated allowing model performance to be accurately evaluated – considering R^2, L1 and L2 correlation parameters. As well as statistical figures, the accuracy of each case can also be graphically displayed - an example of this can be seen above in Figure 12 and Figure 13.

7 MULTIPLE BLADE MODELS

Following the initial surrogate model development for Platform 1, additional work was completed to extend the tools capability to deal with different geometries.

Following the work done in the first stage to develop the surrogate for Platform 1, a new surrogate for a second LH platform (Platform 2) was developed. The tool was also extended to predict data for two further blade designs (similar to those already incorporated).

One of the major advantages of the GCNN neural network used in this work is the ability to generalize data – such that a surrogate model may be improved by training it on multiple geometries and given enough data such a model will be able to accurately predict new, unseen blade geometries.

An initial test of this capability was undertaken as part of this project, training the model on 3 out of 4 of the chosen databases, and then predicting solutions for the final, unseen blade.

8 RESULTS

The following section shows the results and overall performance of the surrogate model developed in this project and presented here. The section is split into two parts considering first the single blade results, and secondly the experimental multi-blade model developed at the end of the project.

Below is a depiction of the reference frame of the helicopter in the following rotor disc plots. The rotor spins anticlockwise, such that the advancing rotor is at the top of the plot.

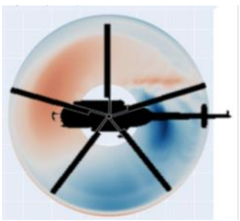

Figure 18: Helicopter reference frame for rotor load contour plots (rotor rotation +ve anti-clockwise)

8.1 Single Blade

The results are displayed in this section for two individual surrogate models, developed for different LH Platforms. The initial investigation was done with Platform 1, presented first. Platform 2, which was developed using an adaptation of the existing pipeline is presented second.

8.1.1 LH Platform 1

The surrogate model was first built and trained on this dataset. Following extensive investigations and development, the final tuned surrogate model produced predictions for each flight condition in the database, with an average test set of r2 values of 99% for rotor thrust (Fz). A heatmap of these r2 values calculated for both test and train sets of the data is shown below in Figure 19.

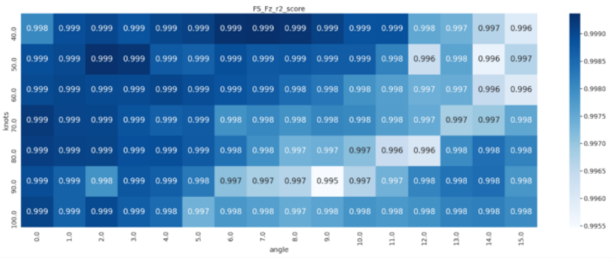

Figure 19: R2 error heatmap for the final platform 1 Fz database predictions

To give a more representative indication on the accuracy of the model predictions, the average absolute error (L1) for Fz has also been plotted in a heatmap, give below in Figure 20. For the two example cases used in the following section (for 70kts, 6º descent and 90kts, 9º descent), the corresponding L1 error was 34N and 57N respectively. This is comfortably within the magnitude of error (or level of uncertainty) expected from the physics based model.

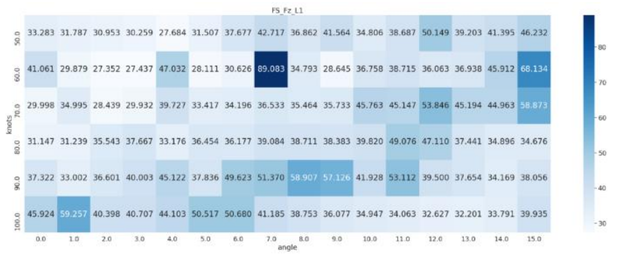

Figure 20: L1 error heatmap for final Platform 1 database Fz predictions

As mentioned in the above sections, the aeroacoustic toolchain is particularly sensitive to small deviations in pressures and pressure gradients. The accuracy of the surrogate model developed for Platform 1 is shown below in Figure 21 and Figure 22 for two example flight conditions, at 70kts 6º descent and 90kts 9º descent respectively.

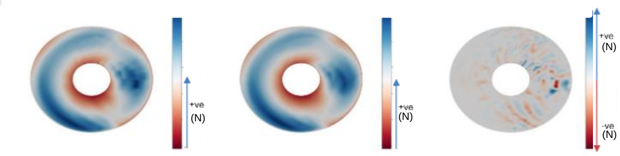

Figure 21: P Fz rotor loads for 70kts, and 6 degree descent for ground truth (left), prediction (centre) and associated error (right)

The results show the close correlation between the physics based model and surrogate predictions, with an average r2 of 0.998 for the 70kts case, and an r2 of 0.995 for the 90kts case. They also show that the remaining errors present in the model are closely correlated with sudden changes in pressure gradient (in this case clearly visible towards the rear of the rotor).

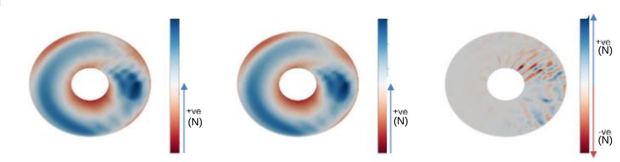

Figure 22: Platform 1 Fz rotor loads for 90kts, and 9 degree descent for ground truth (left), prediction (centre) and associated error (right)

In addition to the rotor thrust distributions, the lift history of the blade through its revolution was also plotted, and used to gauge the performance of the model. Below in Figure 23 and Figure 24 are given the corresponding lift history plots for the rotor loads shown above.

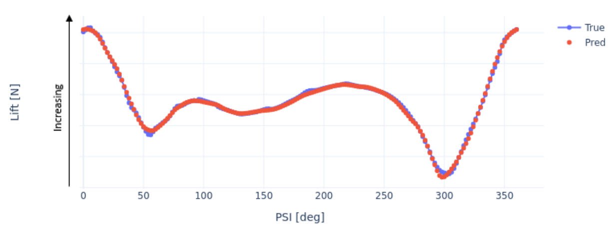

Figure 23: Lift History for Platform 1, 70kts, 6 degree descent

These plots show more clearly the difference in performance between the two flight cases: the 90kts, 9 degree case is clearly slightly less well captured in the regions of significant pressure fluctuation.

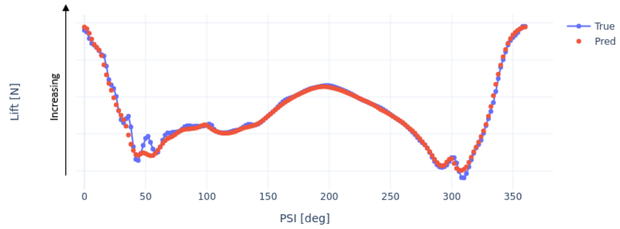

Figure 24: Lift History for Platform 1, 90kts, 9 degree descent

However, even in the case of the more challenging 90kt, 9º descent case, Figure 25 shows that the fine-tuned surrogate model accurately predicts the pressure gradients of the mid fidelity aerodynamics solver. Importantly, the results show that the surrogate model is able to capture the highly non-linear BVI behaviour characteristic of these descent flight conditions (where the rotor wake typically falls into the plane of the rotor).

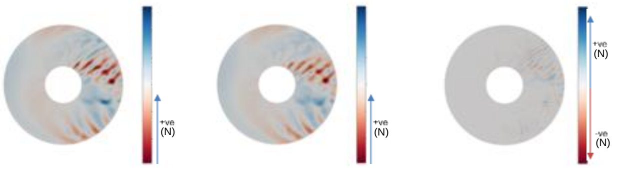

Figure 25: Platform 1 Fz gradients ((Derivative of the Fz with respect to Azimuth Angle), for 90kts, 9 degree descent

The resulting noise hemisphere taken from this case is as shown below in Figure 26. The results show an r2 correlation of 81%, and clearly shows that the directionality and noise level of the helicopter are both maintained by the results – even in the presence of BVI.

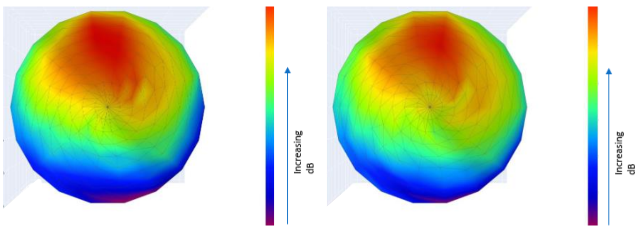

Figure 26: OASPL (Overall Sound Pressure Level) Platform 1 Hemisphere plot (r2 81%), 90kts, 9º descent

8.1.2 LH Platform 2

Following the successful development of a surrogate for Platform 1, an extension activity was performed on a second LH platform. The acoustic database used in this case is shown below in Figure 27.

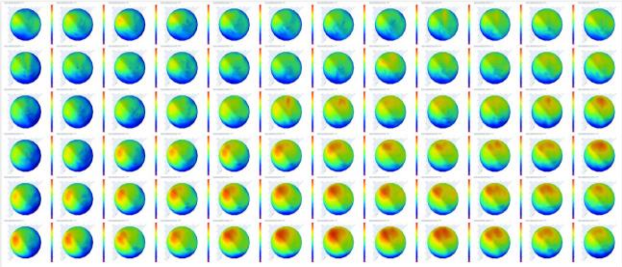

Figure 27: Platform 2 Acoustic Hemisphere Database

Again, the performance of the surrogate model on the full database was evaluated, calculating average r2 and L1 parameters for the Fz distribution of each case, as plotted below in Figure 28 and Figure 29.

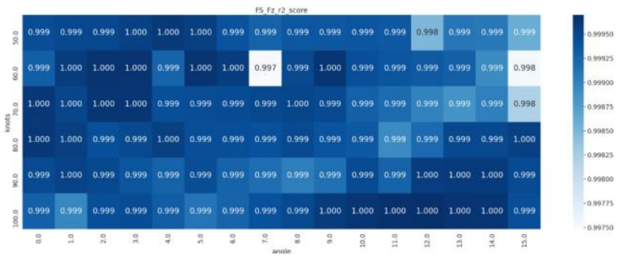

Figure 28: r2 error heatmap for final Platform 2-database Fz predictions

The results show an even stronger correlation between the surrogate and physics based predictions for this platform. The overall results showed an average r2 for each case of 99% for Fz over the rotor. For the two flight conditions considered later on in this section, the same conditions as presented above for Platform 1, the average L1 errors are still 34N and 57N, for the 70kt and 90kt cases respectively. The r2 error for both is 0.999.

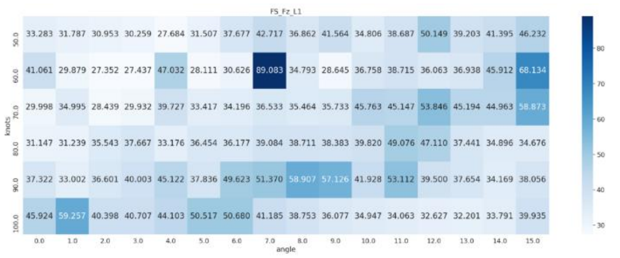

Figure 29: L1 error heatmap for final Platform 2 database Fz predictions

The rotor thrust distributions (on the rotor TPP) for these two flight conditions are shown below in Figure 30 and Figure 31. The results show a very close correlation, with only very minor gradient based errors present. Once again, we can see that the slightly more BVI prone 90kts, 9º condition suffers ever so slightly higher errors.

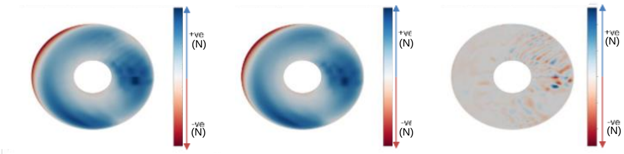

Figure 30: Platform 2 Fz rotor loads for 70kts and 6 degree descent for ground truth (left), prediction (centre) and associated error (right)

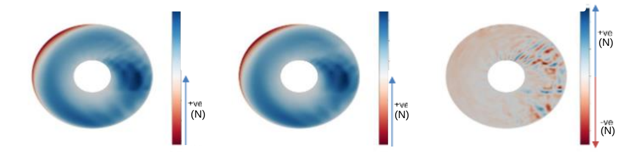

Figure 31: Platform 2 Fz rotor loads for 90kts, and 9 degree descent for ground truth (left), prediction (centre) and associated error (right)

The lift history plots for these flight conditions (see Figure 32 and Figure 33) show a close correlation between surrogate and physics based prediction, even for the lift perturbations present for the 90kts case.

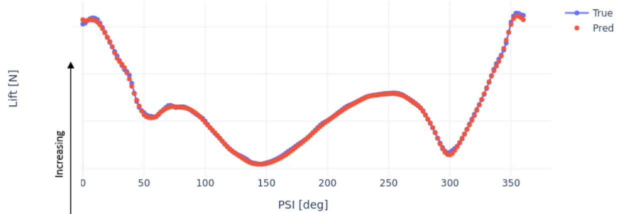

Figure 32: Lift History, Platform 2 70kts, 6 degree descent

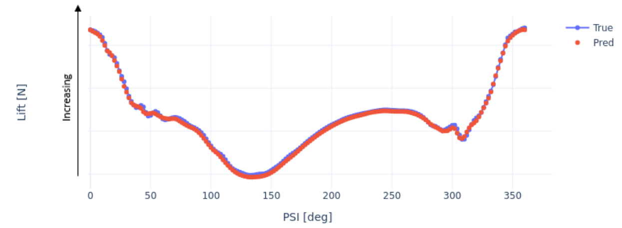

Figure 33: Lift History, Platform 2, 90kts, 9 degree descent

8.2 Multi-blade

In addition to the single blade models developed for two separate LH platforms, an additional investigation was undertaken to consider a multiblade model. In this investigation, 4 datasets were considered, including Platform 1 & 2, and 2 new smaller databases (Platforms 3 & 4) using augmentations of the blade geometry used for Platform 1.

The surrogate model was then trained on Platform 1, Platform 2 and Platform 4. It was then used to predict the unseen second smaller database. Using this model, the test set achieved an average Fz r2 of 99%. The unseen dataset achieved an average r2 of 65%. The r2 for each case in the unseen database are as shown below in Figure 34.

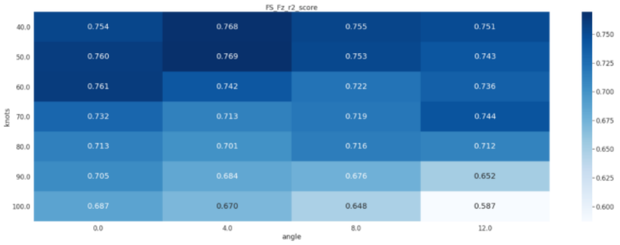

Figure 34: r2 score for the unseen Platform 3 database

However, despite the noticeable reduction in performance of the surrogate model for the unseen data, based on the correlation metric, Figure 35 and Figure 36 show that the majority of this error occurs at the very tip of the blade. The overall lift distribution remains very accurately predicted.

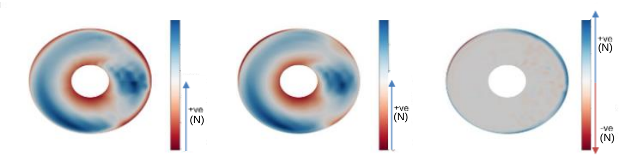

Figure 35: Platform 3 (not seen) Fz rotor loads for 70kts, and 8 degree descent for ground truth (left), prediction (centre) and associated error (right)

This phenomena is confirmed by the lift history plots, shown below in Figure 37 and Figure 38.

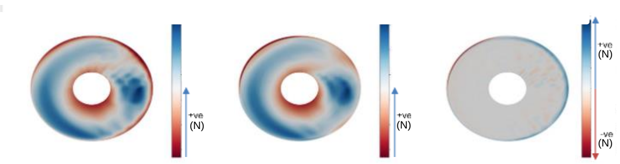

Figure 36: Platform 3 (not seen) Fz rotor loads for 90kts, and 8 degree descent for ground truth (left), prediction (centre) and associated error (right)

These plots show the lift curves for a worst case comparison - a flight condition at 100kts and 12º descent - predicted for the Platform 1 and for the unseen data set. The r2 value for the unseen data set is 58%, while it is 99% for Platform 1 – but the lift curves show that away from the blade tip, the force distribution along the blade remains well resolved. The average unseen data r2 for the lift history plots was 96%, just 1% less than that for the test data set.

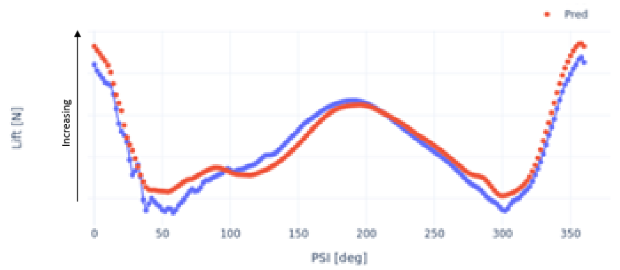

Figure 37: Lift History for the Platform 3, model not trained on the geometry, 100kts, 12 degree descent angle

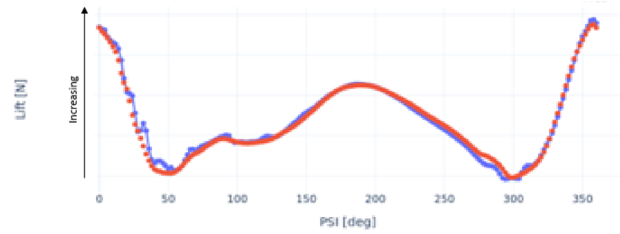

Figure 38: Lift History for the Platform 1, model trained on the geometry, 100kts, 12 degree descent angle

This is corroborated by the rotor thrust distribution contour plots shown below in Figure 39 and Figure 40. The results of this investigation clearly show that the multi-blade model has the potential to be used to predict new blade designs in the future.

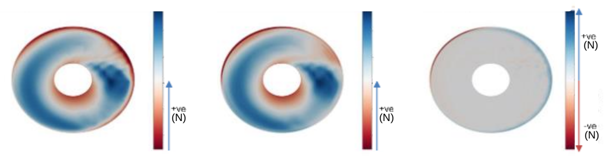

Figure 39: Platform 3 (not seen) Fz rotor loads for 100kts, and 12 degree descent for ground truth (left), prediction (centre) and associated error (right)

With the ingestion of new data, covering a range of blade designs which encompass the types of geometries and flow conditions we expect to encounter with a new blade design, this method has the potential to rapidly predict the performance of new blade designs. Coupled with a powerful optimiser, this method may be able to massively accelerate blade optimisation and design.

Further work needs to be done on this model, to extend its capabilities. It is, of course, limited by the data and flow conditions which it has seen in the datasets it is trained on.

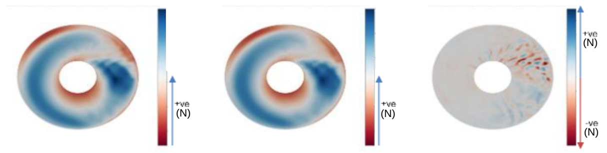

Figure 40: Platform 3 Fz rotor loads for 100kts, and 12 degree descent for ground truth (left), prediction (centre) and associated error (right)

To create an optimisation loop, with morphing geometries and instantaneous performance feedback, the creation of further training data (carefully selected) will need to be undertaken.

9 COMPUTATIONAL PERFORMANCE & NEXT STEPS

Using the new deep learning surrogate model, the time taken to run the full aeroacoustic toolchain is 8 minutes once the model is trained. Using traditional physics based model approaches, the same toolchain could take up to 8 hours to run. This is a game changer for helicopter blade design – and in particular design optimisation. Currently the surrogate model is only limited by the data it has been trained on. Once trained on data covering the full flight envelope of multiple aircraft, the surrogate modelling tool will have the capability to perform morphed geometry optimisations, and give near real time predictions for on-ground noise.

This also gives particular opportunities to enhance customer experiences, allowing mission planning to take into account acoustic helicopter footprints on demand.

10 CONCLUSIONS

This paper has presented a new state of the art surrogate assisted aeroacoustics toolchain. The results have shown that the surrogate model is able to predict the aerodynamic pressure distributions of the rotor in unsteady conditions with a correlation of 99%, for a range of flight speeds and descent trajectories. The surrogate model has been fully integrated within the LH aeroacoustics toolchain, and will be used in tandem with traditional physics based solvers to accelerate LH blade design and development capabilities. It has also been fully deployed on the Davinci1 high performance cluster.

The new surrogate assisted toolchain can run end to end in just 8 minutes, down from the 8 hours taken to run the original aeroacoustics toolchain. In further work, focus will be given to the further training of the surrogate to include flight conditions encompassing the full helicopter flight envelope, and enabling the surrogate to accurately predict new unseen blade performance.

11 REFERENCES

[1] L. M. Cruz, A. S. Melone and A. D'Andrea, "Rotorcraft Multi-Objective Trajectory Optimization for Low Noise Landing Procedures," *European Rotorcraft Forum,* 2012.

[2] G. Sun and S. Wang, "A review of the artificial neural network surrogate modeling in aerodynamic design," *Proceedings of the Institution of Mechanical Engineers, Part G: Journal of Aerospace Engineering,* 2019.

[3] C. Smith, V. Pachidis, A. Pardo, E. Gires, J. Stevens, L. Thevenot and R. d'Ippolito, "Achieving Rotorcraft Noise and Emissions Reduction for 'Clean Sky' - The Measurement of Success," in *Challenges in European Aerospace, 5th CEAS Air & Space Conference*.

[4] N. D. Polyzos, S. Vouros, I. Goulos and V. Pachidis, "Multi-disciplinary optimization of variable rotor speed and active blade twist rotorcraft: Trade-off between noise and emissions," *Aerospace Science and Technology,* vol. 107, 2020.

[5] X. Yan, J. Zhu, M. Kuang and X. Wang, "Aerodynamic shape optimization using a novel optimizer based on machine learning techniques,," *Aerospace Science and Technology,,* vol. 86, pp. 826-835, 2019.

[6] D. Lee, Y.-e. Kang, D.-H. Kim and K. Yee, "Improved Surrogate-based Design Optimization of Composite Rotor Blades," in *American Institute of Aeronautics and Astronautics*, 2022.

[7] D. A. I. J. Forrester, D. A. Sobester and P. A. J. Keane, Engineering Design via Surrogate Modelling: A Practical Guide, 2008.

[8] J. Masci, D. Boscaini, M. M. Bronstein and P. Vandergheynst, "Geodesic Convolutional Neural Networks on Riemannian Manifolds," in *IEEE International Conference on Computer Vision Workshop*, Chile, 2015.

[9] W. J. Vankan, W. F. Lammen and E. H. Baalbergen, "Multidisciplinary Modelling, Analysis and Optimization for Aircraft and System Level Design and Validation," *World Congress in Computational Mechanics (WCCM),* vol. 14th, 2020.

[10] F. Monti, D. Boscaini, J. Masci, E. Rodola, J. Svoboda and M. M. Bronstein, "Geometric deep learning on graphs and manifolds using mixture model cnns," *arXiv preprint arXiv:1611.08402,* 2016.